Spectroscopic Consequences of Localized Electronic Excitation in Anthranilic Acid Dimer

Cathrine A. Southern[†] and Donald H. Levy*

Department of Chemistry and the James Franck Institute, University of Chicago, Chicago, Illinois 60637

Jaime A. Stearns, Gina M. Florio,[‡] Asier Longarte, and Timothy S. Zwier*

Department of Chemistry, Purdue University, West Lafayette, Indiana 47907

Received: January 28, 2004; In Final Form: March 9, 2004

The electronic and infrared spectroscopy of anthranilic acid (*o*-aminobenzoic acid) dimer has been studied in a supersonic jet. Fluorescence-dip infrared (FDIR) spectra have been obtained in both the ground and first excited electronic states. The ground-state FDIR spectrum shows a broad, highly shifted OH stretch absorption commensurate with a cyclic, doubly hydrogen bonded structure, as has been observed for other carboxylic acid dimers. Density functional theory calculations predict that the dimer retains the monomer propensity for the amino group to be adjacent to the carbonyl group of the carboxylic acid, producing a C_{2h} ground-state geometry for the dimer. The presence of the amino group shuts off the double proton tunneling that is present in benzoic acid dimer. The excited-state FDIR spectrum shows NH stretch fundamentals that are the sum of the S_0 and S_1 FDIR spectra of anthranilic acid monomer, indicating that the electronic excitation is localized on one of the monomers in the excited electronic state. The ultraviolet spectrum of the dimer shows a strong Franck−Condon progression involving a 58 cm^{-1} vibration and many combination bands with this mode. Comparison with density functional theory calculations indicates that the 58 cm^{-1} mode involves the in-plane geared bend of the two monomer units, which has b_u symmetry in the C_{2h} ground state. While this non totally symmetric fundamental appears in the R2PI and IR−UV hole-burning spectra, the dispersed fluorescence spectra from the S_1 origin, +58 cm^{-1} band, and +118 cm^{-1} band display intensity only in even members of the 58 cm^{-1} progression. This Franck−Condon activity is quantitatively fit by a model in which the excited-state vibrations are simple sums and differences of localized, shifted harmonic oscillator vibrational wave functions, producing unresolved a_g/b_u tunneling doublets associated with the large barrier that separates the two minima on the excited-state surface.

I. Introduction

Carboxylic acid dimers have been thoroughly examined over the past several decades. The reason for such intense examination is the interest in gaining an understanding of the behavior of systems containing strong intermolecular hydrogen bonds and the possibility of double proton transfer in both the ground and excited states of these systems. Of the many carboxylic acid dimers that have been studied, the benzoic acid dimer is one of the most thoroughly studied. The spectroscopy of this dimer has been investigated in both the crystalline phase[1−4] and the gas phase.[5−10] The structure of this cyclic, hydrogen-bonded dimer is shown in Figure 1a. As anthranilic acid (Figure 1c) contains a carboxyl substituent, it is likely that the dimer of anthranilic acid will form a structure similar to that of benzoic acid dimer. In the ground state, the hydrogen-bonded benzoic acid dimer possesses C_{2h} symmetry. Early studies of benzoic acid dimer in the crystalline phase indicated that electronic excitation of benzoic acid dimer leads to the strengthening of one of the hydrogen bonds, while the other is weakened.[2] Additionally, the dipole−dipole coupling between the monomers

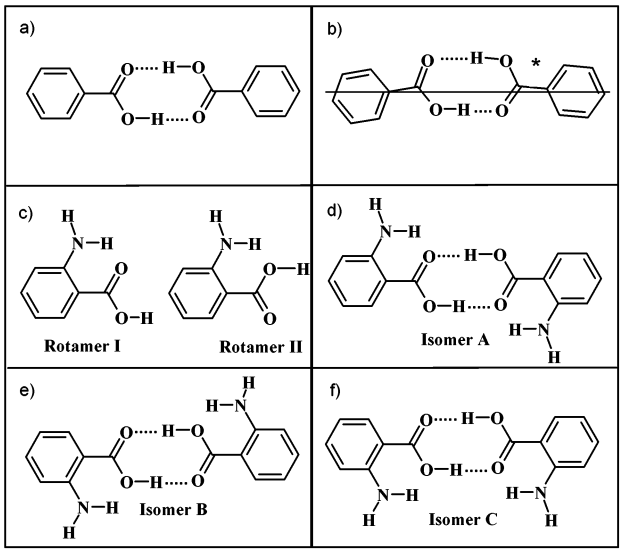

Figure 1. Structures of (a) the cyclic, hydrogen-bonded benzoic acid dimer, (b) the S_1 excited-state benzoic acid dimer, proposed in refs 4 and 6, (c) two rotamers of anthranilic acid monomer, and (d)−(f) three possible isomers for anthranilic acid dimer arising from the rotamer monomer structures. A conclusion of this work is that we only observe isomer A. The asterisk in (b) indicates which monomer is electronically excited.

* Corresponding authors. Phone: (765) 494-5278. E-mail: zwier@purdue.edu. Phone: (773) 702-7196. E-mail: levy@silly.uchicago.edu.

[†] Current address: Department of Chemistry, Amherst College, Amherst, MA 01002.

[‡] Current address: Department of Chemistry, Columbia University, New York, NY 10027.

10.1021/jp0496093 CCC: $27.50
Published on Web 05/05/2004

in the first excited electronic state was calculated to be less than 1 cm^{-1}.[2] With such a weak exciton splitting, even small asymmetries can lead to localized electronic excitation, and the S_1 state of benzoic acid dimer was proposed to be localized on one of the monomeric units in the solid.[2] High-resolution studies of benzoic acid dimer and its deuterated derivatives in the crystalline phase confirmed the occurrence of localized excitation.[4] Taking all of these measurements into account, Baum and McClure concluded that the cause of the localized excitation is the fact that the geometry of the benzoic acid dimer in its first excited electronic state is bent as the result of the differing strengths of the intermolecular hydrogen bonds.[4] A representation of the excited-state geometry predicted by Baum and McClure is depicted in Figure 1b.

In the condensed phase, localized excitation can be caused, at least in part, by the different local environments of the monomers. However, the electronic spectroscopy of benzoic acid[7,8] and *p*-aminobenzoic acid[11] dimers examined in the isolated environment of a supersonic jet has also shown evidence of localized electronic excitation. As in the condensed phase, the primary evidence is that the mixed OH/OD isomer shows two resolvable S_0–S_1 origins due to $C_6H_5COOH^*-C_6H_5COOD$ and $C_6H_5COOD^*-C_6H_5COOH$. This suggests that, even in the absence of solvent effects, the electronic excitation is at least partially localized on one or the other monomer in the excited states.

The results of recent high-resolution electronic spectroscopy on benzoic acid dimer in a supersonic jet[6] support the bent geometry suggested by condensed phase experiments (Figure 1b).[4] The fitted rotational constants are consistent with an excited-state structure that is bent by 3.4° with respect to the longitudinal axis of the dimers.[6] The same high-resolution experiment measured the tunneling splitting associated with double proton transfer in benzoic acid dimer. It is common to call this double transfer a proton transfer rather than a hydrogen transfer, even though the final state is not zwitterionic. We will retain this terminology in what follows in order to distinguish it from the hydrogen transfer involving the NH···O═C group. The measured splitting of 1107 ± 7 MHz does not give the absolute tunneling splitting in either electronic state, but is either the sum or difference of the tunneling splittings in the two states.[6] Whether it is the sum or the difference depends on the relative symmetries of the two states. Previous studies of benzoic acid crystals with two different dopants determined the tunneling splitting in the ground state of benzoic acid dimer to be 8.4 and 6.5 GHz, respectively.[12,13] Remmers et al. assumed that these splittings were similar to that in the isolated molecule, and from this they inferred that the measured 1.107 GHz spectral splitting is the difference between the tunneling splittings in the ground and excited electronic states.[6] This led to the conclusion that the excited-state barrier was either 20% larger or 20% smaller than the ground-state barrier. Based on previous estimates of the ground-state barrier (~1800 cm^{-1}), it is clear that both states possess a relatively large barrier to proton transfer.[6]

In anthranilic acid (AA) dimer, the substitution of an NH_2 group in the ortho position on benzoic acid has several interesting consequences for the electronic structure and excited-state dynamics of the dimer. First, the asymmetric substitution produces two rotamers of the monomer (Figure 1c), which can lead to multiple isomers of the dimer. The rotamers of anthranilic acid monomer are labeled I and II in Figure 1c, in keeping with the notation used for salicylic acid monomer (in which the ortho substituent is OH rather than NH_2).[14,15] If the populations of both rotamers were significant, then a mixture of I−I, II−II, and I−II dimers could be formed (Figure 1d−f). In salicylic acid, the corresponding rotamer I is the dominant isomer observed in the supersonic expansion, and only the I−I dimer structure (isomer A) is observed. This was determined by a recent fluorescence-dip infrared experiment[14] in which the experimental spectrum was compared to the infrared spectra of isomers A and B calculated at the B3LYP/6-31G(d, p) level.[14] One anticipates a similar circumstance in AA dimer, since only rotamer I of AA monomer was observed in the supersonic expansion.[16]

Second, substitution in the ortho position leads to an asymmetry in the double minimum well for proton transfer involving the carboxylic acid hydrogens, shutting off the tunneling pathway for interdimer double proton transfer near the zero-point level.

Finally, the AA monomer shows evidence of undergoing a hydrogen "dislocation" in its first excited singlet state that moves it partway from the amine to the imine tautomeric form.[16] This dislocation involves a substantial geometry change for the entire chelating ring involved in the intramolecular hydrogen bond.[16,17] It is a main goal of the present study to determine the extent to which the structural distortion in the monomer leads to localization of the electronic excitation in the excited state of the dimer. If the distortion does localize the electronic excitation, we seek to observe and understand the spectroscopic consequences of that localization. The typical signature of H-atom or proton transfer is a red shift in the emission from the excited state. In salicylic acid dimer, the decrease in the magnitude of this shift relative to that in the monomer was used by Lahmani et al. to deduce that dimerization weakens the intramolecular hydrogen bond in salicylic acid due to the presence of the intermolecular hydrogen bonds.[18]

While the shift in the emission is a useful probe of the excited-state geometry, it does not give specific information regarding the type of structural change induced. Furthermore, it can lead to ambiguity as the magnitude of the red shift decreases in size. In the present study we probe the hydrogen atom dislocation via hydride stretch infrared spectroscopy in the excited electronic state. The spectra obtained show direct evidence for electronic localization in the excited state. In addition, the vibronic spectroscopy exhibits a subtle but no less important signature of electronic localization in the Franck−Condon progressions associated with the intermolecular geared bending mode.

II. Experimental Section

Anthranilic acid dimer was studied by means of dispersed emission, two-color resonance-enhanced two-photon ionization (R2PI), ground- and excited-state fluorescence-dip infrared (FDIR), and IR−UV hole-burning spectroscopies. Brief descriptions of each technique follow.

A. Dispersed Emission. The apparatus used to obtain the dispersed emission spectra has been described previously[19] and will be described only briefly here. The sample was heated to 150 °C to attain a sufficient vapor pressure; the nozzle temperature was kept about 15 °C higher than the sample temperature. The molecules were seeded into helium gas at a stagnation pressure of 3−4 bar, and the mixture was expanded into a vacuum chamber through a 50 μm orifice. The supersonic expansion was crossed with the frequency-doubled output of an Nd:YAG-pumped dye laser approximately 5 mm downstream of the nozzle. Dispersed emission spectra were recorded by exciting a particular transition and detecting the fluorescence with a photomultiplier tube after dispersing it through a monochromator with a dispersion of 4 Å/mm.

B. Two-Color R2PI. To obtain the R2PI spectrum, a reflectron time-of-flight mass spectrometer, which has been described previously, was used.[20] The ionization potential of anthranilic acid dimer is too large for one-color resonant two-photon ionization. Ionization was achieved by introducing the fourth harmonic of another Nd:YAG laser (266 nm) in a counter-propagating geometry. The relative timing between the two lasers was controlled with a digital delay generator (SRS DG535). Optimum signal was obtained for zero time delay between the two lasers. The two-color R2PI spectrum was obtained by gating the detector on a particular mass and scanning the UV laser to observe the wavelengths at which enhanced signal was observed.

C. Fluorescence-Dip Infrared Spectroscopy.[21−23] Conformation-specific infrared spectra in the ground and excited electronic states were obtained using fluorescence-dip infrared (FDIR) spectroscopy. A seeded Nd:YAG-pumped optical parametric converter (LaserVision, KTA based, 10 Hz) was used to produce tunable IR radiation from 2200 to 4000 cm^{-1}. Infrared laser powers of 1−3 mJ/pulse were typical. The UV and IR laser beams were spatially overlapped approximately 5 mm from the pulsed valve, and temporally separated by approximately 100 ns, with the IR preceding the UV. To generate the ground-state FDIR spectrum, the UV laser was fixed to a particular vibronic transition in the fluorescence excitation spectrum and the total fluorescence signal was monitored. Whenever the parametric converter was resonant with an infrared transition in the hydride stretching region, population was removed from the ground vibrational state, which resulted in a depletion in the total fluorescence signal from that level when the UV laser interrogated it. Depletions were recorded by comparing the total fluorescence signal with and without the IR laser present using active baseline subtraction.

In the excited-state FDIR experiment, the UV laser precedes the IR laser by 10−15 ns. The UV laser was tuned to a known transition in the R2PI spectrum. The IR laser then promoted the molecule to higher lying vibrational levels within the excited electronic state. The rate of radiationless processes in the molecule is more rapid at these levels, causing a decrease in the fluorescence quantum yield relative to that of the initially excited level. By detecting the fluorescence signal with a gate positioned late in the fluorescence decay, the infrared absorptions are detected as depletions in the fluorescence signal when the IR laser is resonant with a vibrational transition in the excited electronic state. In a fashion similar to that of the ground-state FDIR technique, the subtraction of the total fluorescence signals with and without the IR laser present generated the excited-state FDIR spectrum.

D. IR−UV Hole-Burning Spectroscopy. In contrast to FDIR spectroscopy, which tunes the infrared laser while fixing the UV laser, IR−UV hole-burning spectroscopy fixes the IR laser to a unique IR transition of the dimer while tuning the UV laser through the laser induced fluorescence (LIF) transitions of interest. Only LIF transitions that share the same ground-state level with this IR transition will appear in the difference spectrum (IR laser on − IR laser off).

E. Calculations. Density functional theory (DFT) calculations using the Becke3LYP functional with a 6-31G(d,p) basis set were carried out on the ground electronic state of anthranilic acid dimer to provide a basis of comparison with experimental results. Fully optimized structures, harmonic frequencies, and IR intensities were calculated for the three isomers of anthranilic acid dimer shown in Figure 1d−f. All calculations were carried out using the Gaussian 98 suite of programs.[24]

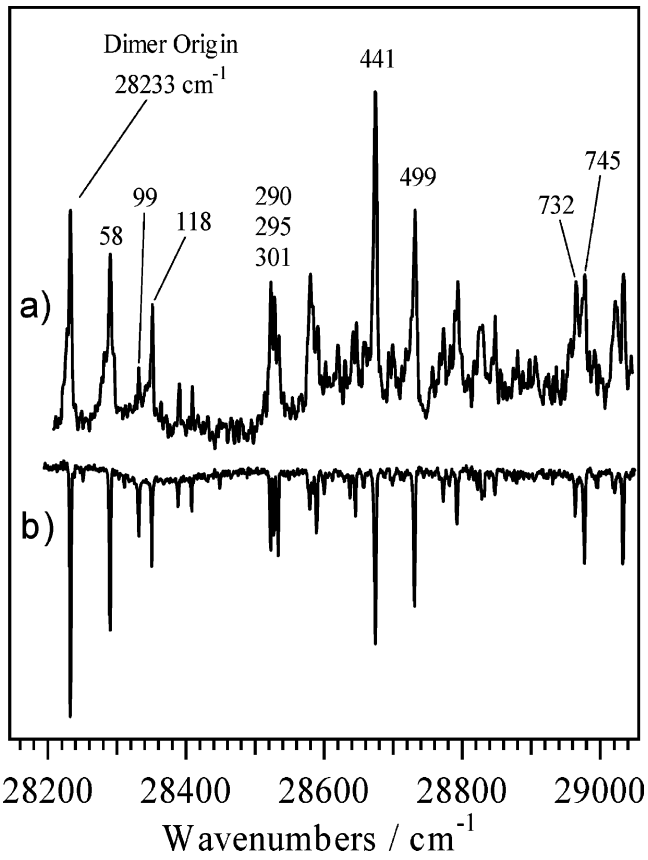

Figure 2. (a) R2PI spectrum and (b) IR−UV hole-burning spectrum of AA dimer. The $S_1 \leftarrow S_0$ origin occurs at 28 233 cm^{-1}.

III. Results and Analysis

A. Electronic Spectroscopy. The two-color R2PI spectrum of anthranilic acid dimer is shown in Figure 2a, while the IR−UV hole-burning spectrum is shown in Figure 2b. The hole-burning spectrum was recorded with the IR laser fixed at 3000 cm^{-1}, at the peak of the H-bonded OH stretch of the dimer (section III.C). The IR−UV hole-burning scan is somewhat less saturated than the R2PI spectrum because the LIF probe signal could be obtained with adequate intensity at somewhat lower laser fluence. The feature at 28 233 cm^{-1} is assigned to the dimer origin, which is red-shifted 349 cm^{-1} relative to the anthranilic acid monomer origin.[16] No other features were observed to the red of this band. The red shift observed is similar to the 237 cm^{-1} red shift of the benzoic acid dimer origin relative to that of the monomer.[25]

Most of the vibronic structure in the spectrum can be accounted for by progressions and combination bands involving three intervals of 58, ∼290, and 440 cm^{-1}. The band near 290 cm^{-1} is actually a triplet of transitions (best seen in Figure 2b) at 290, 295, and 301 cm^{-1}. We will return to a discussion of this splitting after considering the calculated vibrational modes. As we shall see in section III.E, the 290 and 440 cm^{-1} transitions have close analogues in the dispersed emission scans, which can be assigned to in-plane bending modes of the NH_2 and COOH groups.[16]

The strong vibrational progression with a spacing of 58 cm^{-1} dominates the low-energy region of the spectrum, with bands appearing at 58, 118, and 176 cm^{-1}. Many other vibronic

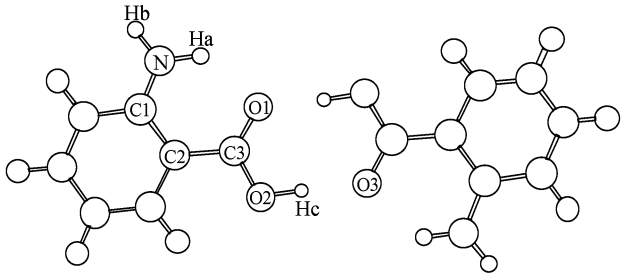

Figure 3. Minimum energy calculated structure (B3LYP/6-31G(d,p)) of AA dimer in its ground electronic state, isomer A. The atomic labels shown are relevant for the geometric parameters given in Table 1.

TABLE 1: Calculated Geometric Parameters for Anthranilic Acid Monomer and Dimer

calculated parameters[a]	anthranilic acid (rotamer I)	anthranilic acid dimer (isomer A)
R_{N-Ha}	1.012 Å	1.011 Å
R_{N-Hb}	1.006 Å	1.006 Å
$R_{O1\cdots Ha}$	1.924 Å	1.925 Å
R_{O2-Hc}	0.971 Å	1.005 Å
$R_{O2\cdots O3}$		2.639 Å
R_{C3-O1}	1.229 Å	1.250 Å
D_{CCNHa}	8.5°	9.4°
D_{CCNHb}	−12.1°	−12.7°
$\theta_{Hb-N-Ha}$	120.1°	119.9°
$\theta_{Ha-N-C1}$	117.7°	117.7°
$\theta_{N-C1-C2}$	122.0°	122.4°
$\theta_{C2-C3-O1}$	126.1°	123.1°
$\theta_{C1-C2-C3}$	120.1°	121.3°
$\theta_{C3-O2-H1}$	105.2°	110.2°

[a] Calculations were performed at the B3LYP/6-31G(d,p) level. Atomic labels are defined in Figure 3.

transitions display combination bands with this mode. A 58 cm^{-1} mode has been observed previously in supersonic jet studies of benzoic acid[7,9] and salicylic acid dimers,[15] both of which are bound together by two intermolecular hydrogen bonds between the carboxyl groups of the monomer units (Figure 1a). Based on density functional theory (DFT) calculations at the B3LYP/6-31+(d) level,[5] Florio et al. assigned the 58 cm^{-1} mode of benzoic acid dimer in its electronic ground state to the in-plane gearing motion of the monomer units. The fact that this mode is also observed in anthranilic acid dimer suggests that the structure of anthranilic acid dimer involves the same hydrogen-bonding geometry that is present in benzoic acid and salicylic acid dimers.

B. Calculations. As mentioned in the Introduction, there are two possible rotamers of AA monomer, leading to three possible isomers for the hydrogen-bonded dimer (Figure 1d−f). DFT calculations at the B3LYP/6-31G(d,p) level were performed on all three dimer isomers to determine the lowest energy structure. These results indicate that isomer A (calculated structure shown in Figure 3) is more stable than isomers B and C by 2.89 and 1.72 kcal/mol, respectively, including zero-point energy corrections. The greater calculated stability of isomer A (the I−I dimer), when coupled with the dominance of rotamer I in the jet, lead us to conclude that isomer A is the form of AA dimer present in the supersonic jet. Therefore, this structure is assumed in the assignments of the observed vibronic features.

A comparison of the calculated geometric parameters of the ground state of AA dimer (isomer A) with those of rotamer I of the monomer is given in Table 1. The carboxyl group, as expected, is most affected by dimerization. This is indicated by the increase in the C═O and OH bond lengths. The intermolecular hydrogen bond lengths of AA dimer, 2.639 Å, are similar to those calculated for salicylic acid dimer, 2.645 Å.[14] In the ground state, the geometry of the anthranilic acid amino group does not substantially alter upon dimerization, as shown by the small decrease in the NH_a bond length and the small increase of the $NH_a\cdots O$ distance. In salicylic acid, the effect of dimerization on the intramolecular hydrogen bond is considerably greater.[14] This is an indication that the intramolecular hydrogen bond in anthranilic acid is quite weak in the ground state, as was observed in the FDIR spectrum of AA monomer.[16]

TABLE 2: Frequencies of Selected Ground- and Excited-State Vibrations of Anthranilic Acid Dimer

S_0/ cm^{-1}	calculated[a]/ cm^{-1}	S_1/cm^{-1}	assignment
58	58	58	ip geared bend
	104		ip shear
110	118	99	ip H-bond stretch
		158	99 + 58
		177	118 + 58
292	307/308	290/295/301	ip COOH bend
		347/358	290/301 + 58
440	443	441	NH_2 ip bend, either C═O ip bend or COOH-ring stretch
		499	441 + 58
548	573/576	560	6a[b] or 118 + 441
730		732	mixed modes involving O−C═O bend and ring distortion
		745	
		790	
		801	

[a] Calculations were performed on the ground state of anthranilic acid dimer at the B3LYP/6-31G(d,p) level. Frequencies have not been scaled. [b] Based on Wilson's notation for the vibrations of benzene.[26]

To aid in assigning the observed vibrational features, harmonic vibrational frequencies were calculated for isomer A using density functional theory at the B3LYP/6-31G(d,p) level. As these calculations were performed on the ground state of AA dimer, the comparison of the calculations with the observed emission spectra is most valid. After the emission spectra have been assigned, comparisons may be made with the R2PI spectrum in order to assign the features present there. In all cases, previous assignments for related molecules were also used. Table 2 lists selected vibrations observed in the R2PI and emission spectra, as well as calculated values and normal mode assignments for these vibrations. The low-frequency vibrations (<200 cm^{-1}) are due to the six intermolecular modes of the dimer. The higher energy vibrations (>200 cm^{-1}) usually occur in closely spaced pairs, typically split by a wavenumber or less, which correspond to the in-phase and out-of-phase combinations of the monomer modes. For instance, the in-plane monomer vibrations generate an a_g/b_u pair in the dimer, if C_{2h} symmetry is preserved. However, only the a_g symmetry vibrational levels will have dipole-allowed transitions from the zero-point level of the ground state. Furthermore, vibronic coupling of the b_u member of the tunneling doublet can only occur to the A_g excited state, which also is symmetry forbidden in transitions from the ground state. As a result, the observed splittings of some of the bands in the spectrum (e.g., the triad of peaks at 290/295/301 and the doublets at 732/745 and 790/801) must be due to anharmonic mixing between a_g vibrational levels in the B_u excited state.

C. Fluorescence-Dip Infrared (FDIR) Spectroscopy. The ground-state FDIR spectrum of anthranilic acid dimer obtained by fixing the UV laser at the dimer origin (28 233 cm^{-1}) is shown in Figure 4a. Two sharp transitions are observed at 3407 and 3545 cm^{-1}, which can be attributed to the NH stretch fundamentals of the dimer. These appear very close to the AA

TABLE 3: Comparison of Observed and Calculated Hydride Stretch Frequencies of Anthranilic Acid Dimer[a]

observed	calculated (isomer A)		calculated (isomer B)		
freq	freq	intensity	freq	intensity	assignment[b]
3407	3399	190	3431	149	symm NH_2 stretch
3545	3550	139	3559	149	asymm NH_2 stretch
3000[c]	2998	6902	2827	8225	OH stretch

[a] Calculations were performed at the B3LYP/6-31G(d,p) level. Frequencies have been scaled by a factor of 0.9528. [b] All frequencies are given in units of cm^{-1}; integrated intensities are in units of km/mol. The dimer hydride stretches are the out-of-phase combinations of the monomer vibrations. [c] The value given is the approximate center frequency of the 650 cm^{-1} broad band.

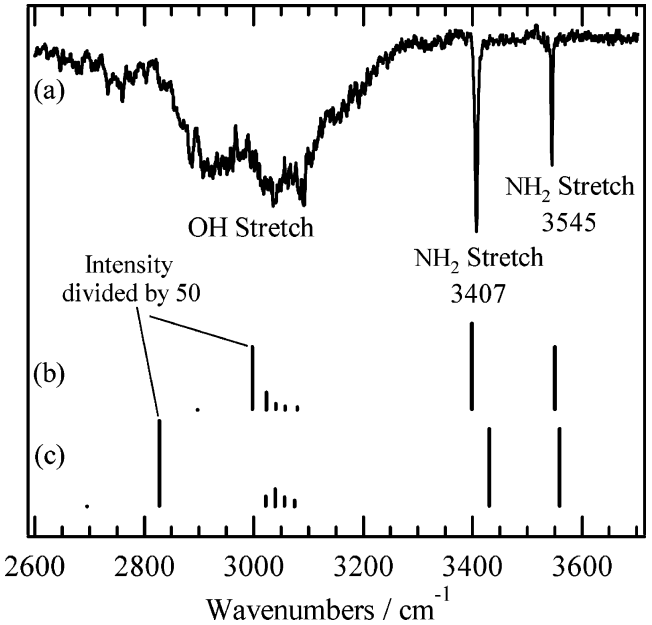

Figure 4. Comparison of (a) observed ground-state FDIR spectrum of anthranilic acid dimer with B3LYP/6-31G(d,p) calculated IR spectra of (b) dimer isomer A and (c) dimer isomer B. The calculated XH stretch frequencies are scaled by a factor of 0.9528. The intensities of the calculated OH stretches have been divided by a factor of 50 so that the other calculated modes are visible.

monomer ground-state values (3394 and 3542 cm^{-1}) for the NH_2 symmetric and antisymmetric stretch fundamentals, respectively. Since there are two NH_2 groups in the dimer, an asymmetric structure would produce four NH stretch fundamentals. However, if the dimer retains C_{2h} geometry, only two of these normal modes would have allowed fundamentals (with b_u symmetry), namely, the out-of-phase combination of the monomer symmetric and antisymmetric stretches, occurring at 3407 and 3545 cm^{-1}, respectively. The observation of only two NH stretch fundamentals in the dimer removes the C_s symmetry dimer (isomer C) from consideration, since it would have four unique, allowed NH stretch fundamentals.

The most prominent feature in the ground-state FDIR spectrum is the broad, intense band centered at approximately 3000 cm^{-1}. This band covers a range of 650 cm^{-1}, extending from approximately 2600 to 3250 cm^{-1}. A similar band has been observed in the FDIR spectra of both benzoic acid[5] and salicylic acid[14] dimers, and has been attributed to the out-of-phase combination (b_u symmetry) of the hydrogen-bonded OH stretches. The frequency of this OH stretch is red shifted by approximately 600 cm^{-1} from the OH stretch observed in anthranilic acid monomer, which occurs at 3592 cm^{-1}.[16] This extreme red shift, as well as the breadth and intensity of this band, is characteristic of strongly hydrogen bonded dimers.

To confirm the assignments given above, the experimental ground-state infrared spectrum was compared to the calculated results, which have been scaled by a factor of 0.9528. The IR spectra of isomers A and B (structures shown in Figure 1d,e) predicted by harmonic frequency calculations at the B3LYP/6-31G(d,p) level are shown in Figures 4b,c. The comparison of the calculated frequencies and intensities with the experimental values is presented in Table 3. The calculations indicate that the IR band observed at 3407 cm^{-1} corresponds to the out-of-phase combination of the symmetric NH_2 stretches of the monomers, while the band at 3545 cm^{-1} corresponds to the out-of-phase combination of the antisymmetric NH_2 stretches of the monomers.[16] The symmetric stretch mode is more affected by dimerization than the antisymmetric mode; it is blue shifted by 13 cm^{-1} relative to the monomer. This blue shift is presumably caused by the weakening of the intramolecular HNH···O═C hydrogen bonds due to the intermolecular hydrogen bonds present in the dimer.

The experimental spectrum agrees better with the calculated spectrum for isomer A than that calculated for isomer B, although one could not make a distinction between the two based solely on this comparison. Nevertheless, this comparison provides confirming evidence that isomer A is responsible for the dimer features observed in the jet spectrum, as indicated earlier by the fact that this is the lowest energy conformation. It is interesting to observe, based on the red shift and intensity of ν_{OH} predicted by the calculations, that the intermolecular hydrogen bonds in isomer B are stronger than those in isomer A. This is consistent with the calculated binding energy for isomer B (21.5 kcal/mol, zero-point energy corrected) being greater than that for isomer A (18.1 kcal/mol). This suggests that isomer B is not present in the expansion only because rotamer II of the monomer is not present, with a calculated energy 2.89 kcal/mol above rotamer I.

As the calculated infrared spectra are obtained under the harmonic approximation, they do not reproduce the breadth observed in the experimental spectrum for the OH stretch. Instead, a single, intense band is predicted for the out-of-phase combination of the OH stretches. The examination of benzoic acid dimer by Florio et al. indicated that the breadth of the OH stretch band was due to strong anharmonic coupling between the OH stretch and bend modes.[5,27] As the same hydrogen bonds are present in anthranilic acid dimer, the breadth of the OH feature in the IR spectrum for anthranilic acid dimer is presumably due to the same anharmonic coupling. Florio et al. were able to replicate the general features of the experimental spectrum by applying a model that included cubic anharmonic coupling terms in the calculation of the infrared spectrum of benzoic acid dimer.[5,27] It is likely that the application of the same procedure for anthranilic acid dimer would account in a similar way for the breadth and substructure of the experimental infrared spectrum, but such a calculation has not been carried out.

D. Excited-state FDIR Spectroscopy. The same broad OH feature is observed in the excited-state FDIR spectrum, which is shown in comparison to the ground-state FDIR spectrum in Figure 5. While the OH stretch feature remains relatively

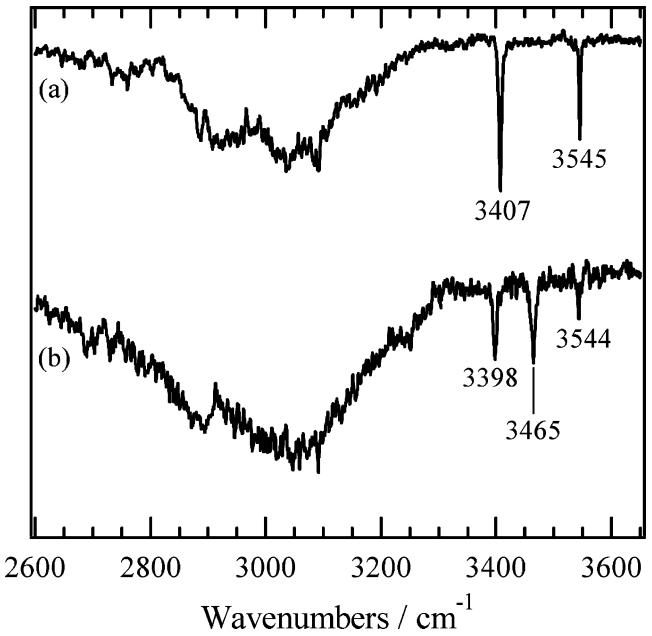

Figure 5. Comparison of (a) ground- and (b) excited-state FDIR spectra of anthranilic acid dimer. The labeled features correspond to NH stretching modes.

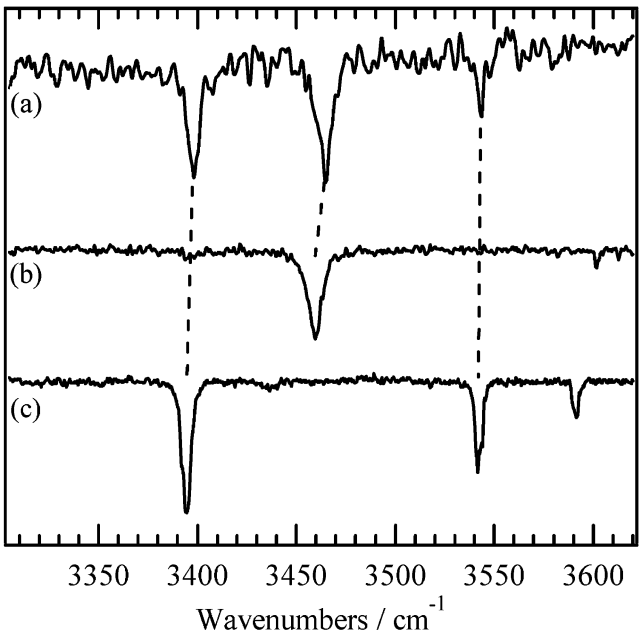

Figure 6. Comparison of NH stretch regions of (a) excited-state FDIR spectrum of anthranilic acid dimer, (b) excited-state FDIR spectrum of anthranilic acid monomer, and (c) ground-state FDIR spectrum of anthranilic acid monomer.

unchanged in the excited-state spectrum, the NH stretch region shows three bands, whereas only two were observed in the ground-state FDIR spectrum. These three stretches occur at 3394, 3465, and 3544 cm^{-1}. The comparison of the NH stretch region of the excited-state dimer spectrum with both the ground- and excited-state monomer FDIR spectra is shown in Figure 6.

The symmetric and antisymmetric NH_2 stretches of the ground-state monomer (Figure 6c) occur at 3394 and 3542 cm^{-1}, respectively. By contrast, there is only one NH stretch present in this region in the excited-state FDIR spectrum of anthranilic acid monomer (Figure 6b). This occurs because the intramolecular hydrogen bond of the monomer is strengthened in the excited electronic state due to hydrogen "dislocation", causing

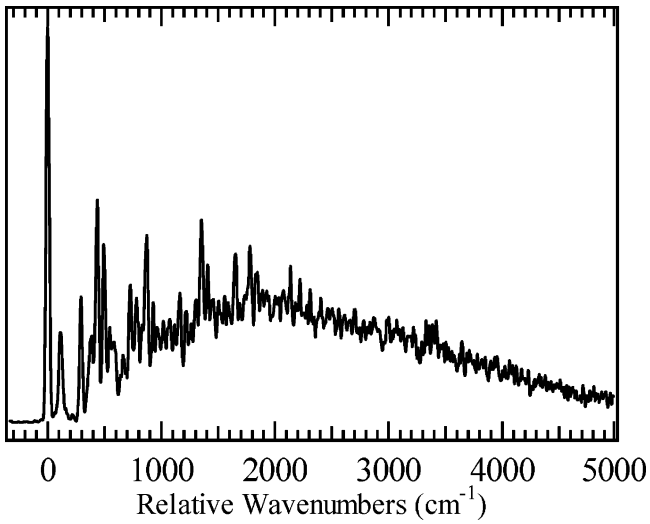

Figure 7. Dispersed emission spectrum that results from exciting the origin transition of AA dimer. The absolute wavenumber position of the origin transition is 28 233 cm^{-1}. The contribution of scattered light to the signal at the excitation wavelength is negligible. The spectral resolution is 0.4 nm (22−32 cm^{-1}).

the two NH oscillators to decouple. The band at 3460 cm^{-1} is attributed to the stretching motion of the "free" NH group not involved in the intramolecular hydrogen bond. The "dislocated" NH stretch fundamental is shifted to considerably lower frequencies, and was tentatively assigned to a weak, broadened transition at 2900 cm^{-1}.[16]

Figure 6 highlights the striking fact that the entire NH stretch region of the excited-state FDIR spectrum of anthranilic acid dimer (Figure 6a) appears to be a simple sum of the ground- and excited-state FDIR spectra of anthranilic acid monomer (Figure 6b,c). In particular, the positions of the outer two bands in Figure 6a are within a few wavenumbers (3398, 3544 cm^{-1}) of the symmetric and antisymmetric NH_2 stretch fundamentals of the ground-state monomer (3394, 3544 cm^{-1}). At the same time, the transition at 3465 cm^{-1} in the dimer excited state spectrum is virtually identical in frequency and band shape to the free NH stretch fundamental of the excited-state monomer. This is a clear indication that the electronic excitation is localized on one of the monomers, so that one has NH stretch fundamentals characteristic of the AA monomer excited state, while the other is essentially unperturbed from its ground-state values. The fourth NH stretch fundamental due to the dislocated NH stretch is anticipated to occur near 2900 cm^{-1}, if the presence of the other AA monomer has only a minor effect on the dislocation. Indeed, a small shoulder on the main OH stretch band is observed in this region. However, the presence of the strong, broad OH stretch absorption in this region prevents a clear assignment.

E. Dispersed Emission Scans. An overview emission spectrum that results from excitation of the origin transition at 28 233 cm^{-1} is shown in Figure 7. Most of the vibronic structure can be accounted for as progressions and combination bands with spacings of 116, 292, and 440 cm^{-1}. These long Franck−Condon progressions lead to a dense, congested spectrum with a maximum approximately 1800 cm^{-1} above the origin. This is similar to, but slightly less than, the maximum found in the monomer (2400 cm^{-1}).[16] In systems capable of proton or hydrogen atom transfer, the magnitude of this shift is taken as an indicator that transfer has occurred. For example, in 7-azaindole dimer, which undergoes a double proton transfer in the excited state, the emission maximum is red shifted by 10 000

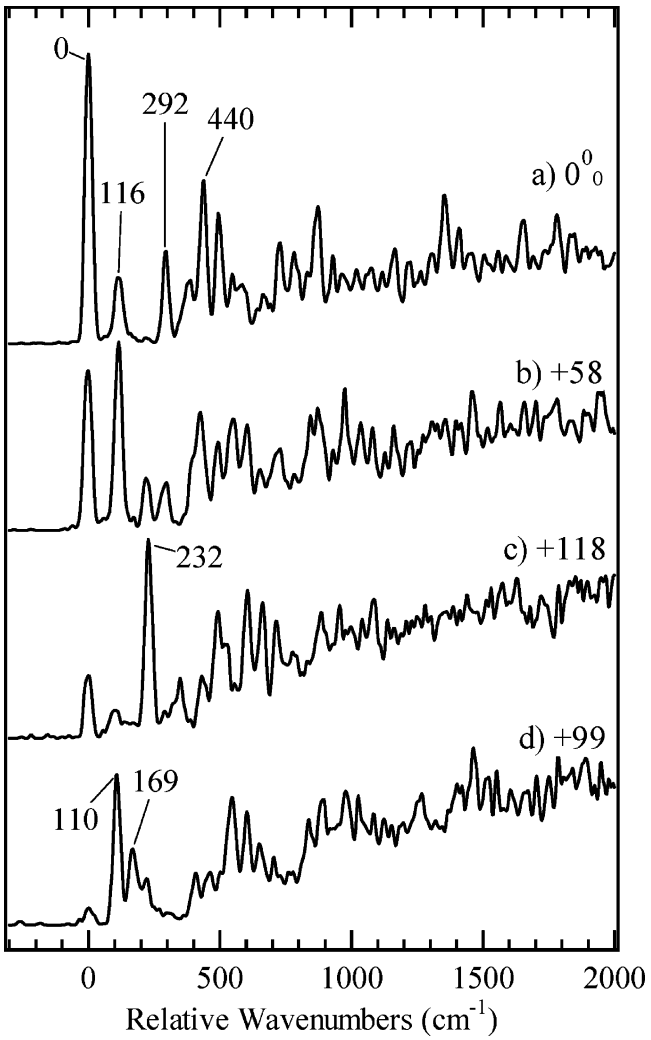

Figure 8. Dispersed emission spectra that result from exciting the (a) origin transition and transitions (b) 58, (c) 118, and (d) 99 cm^{-1} above the origin in AA dimer. The spectral resolution in all scans was 0.4 nm (22−32 cm^{-1}). The contribution to the signal at the excitation wavenumber (relative wavenumber = 0) is 0, 15%, 35%, and 100% for spectra a, b, c, and d, respectively.

cm^{-1}.[28−31] In supersonic jet studies of salicylic acid monomer, a red shift of approximately 6500 cm^{-1} has been observed.[15,32] The theoretical calculations of Sobolewski and Domcke indicate that this red shift is a result of a partial transfer, termed a "hydrogen dislocation" between the ortho OH and carboxylic acid carbonyl groups.[33,34] This red shift is reduced to 3000 cm^{-1} in salicylic acid dimer, which has been interpreted as a reduction in the geometry change experienced by the atoms in the intramolecular hydrogen-bonded ring due to the intermolecular hydrogen bonds formed in the dimer.[18] The smaller magnitude of the red shifts in AA monomer (2400 cm^{-1}) and dimer (1800 cm^{-1}) suggest a smaller dislocation in the monomer, with a correspondingly smaller reduction induced by dimerization.

Spectra a, b, c, and d of Figure 8 present the low-energy region of a series of dispersed emission scans following excitation of the origin and the transitions 58, 118, and 99 cm^{-1} above the origin, respectively. As already mentioned, the most intense transitions in Figure 8a are at 292 and 440 cm^{-1} above the origin. By comparison, the corresponding bands in AA monomer had frequencies of 252 and 410 cm^{-1}. In an earlier work on AA monomer, the 252 cm^{-1} mode was assigned to the in-plane bend of the carboxyl group, while the 410 cm^{-1} mode involves the in-plane bends of the amino and carbonyl groups.[16] The Franck−Condon activity in these modes reflects the change in geometry in the H-bonded chelating ring associated with the hydrogen dislocation. The fact that these vibrations increase in frequency in the dimer indicates stiffening in the bending potentials of these groups in response to the formation of the intermolecular carboxylic acid hydrogen bonds. The calculated, unscaled harmonic vibrational frequencies reflect this change, shifting from 248 to 307 cm^{-1} and from 420 to 442 cm^{-1}, respectively, upon dimerization. A second vibration with a calculated vibrational frequency of 443 cm^{-1} corresponds to the 6a ring deformation, which may contribute to the intensity of the 440 cm^{-1} band as well.

The other striking feature of Figure 8a is that the first band in the emission spectrum appears at 116 cm^{-1}, a factor of 2 greater than the 58 cm^{-1} band observed in the R2PI spectrum (Figure 2a). Furthermore, when the transitions 58 and 118 cm^{-1} above the origin are excited (Figure 8b,c), clear changes in the intensity of transitions at 0, 116, and 232 cm^{-1} occur, but in no case is there any evidence of transitions at 58 or 176 cm^{-1} (i.e., odd multiples of 58 cm^{-1}). The 58 and 118 cm^{-1} bands in the excitation spectrum were tentatively identified in section III.B as the fundamental and first overtone of the geared intermolecular bend, a b_u symmetry vibration (in C_{2h}) with a calculated frequency of 60 cm^{-1}. If the AA dimer were to retain the C_{2h} symmetry in the electronic transition, the b_u fundamental would not be allowed either in excitation or in dispersed emission. However, the observation is that this fundamental is observed clearly in the excitation spectrum, but is absent from the emission spectra.

The excited-state FDIR spectrum provides clear evidence that the excited-state vibrational wave functions of the NH stretch modes are localized on the monomer subunits, with one set of NH stretch fundamentals reflecting a local electronic environment like the ground electronic state of the monomer, while the other set of NH stretch fundamentals reflects an excited electronic state local environment. The question is whether this electronic localization also manifests itself in the anomalous vibronic structure in the progressions of the geared intermolecular bend.

Early attempts at fitting the Franck−Condon intensities for the set of excitation and dispersed emission scans using a shifted, harmonic excited-state well for the geared intermolecular bend were unsuccessful. Attempts were made with $\delta = (\omega'/\omega)^{1/2} = 1$ or $1/\sqrt{2}$,[35] without even qualitative success in the fitting. However, the model of a single, shifted harmonic well in the excited state is not correct. In the next section, we present an alternative model that accounts for the observed Franck−Condon profiles for the geared intermolecular bend.

We note that the emission spectrum shown in Figure 8d (excitation of the +99 cm^{-1} band) is anomalous. This spectrum has a false origin at +110 cm^{-1} and does have a feature displaced by 59 cm^{-1} from the false origin.

F. Exciton Theory in the Presence of Large Intramolecular Geometry Changes. *1. The Electronic Wave Functions.* Exciton theory typically uses products of the monomer electronic wave functions as basis functions for the description of the excited states of a homodimer. The reader is referred to the recent paper by Müller et al. for a useful introduction to exciton theory and its application to the pyridone dimer.[36] If we label the electronic wave functions for monomers "a" and "b" as ψ_a and ψ_b, respectively, then the ground-state wave function for the dimer is $\Psi_{gd} = |\psi_a\rangle|\psi_b\rangle$. The close-lying pair of excited states in the dimer will have excited-state character that depends

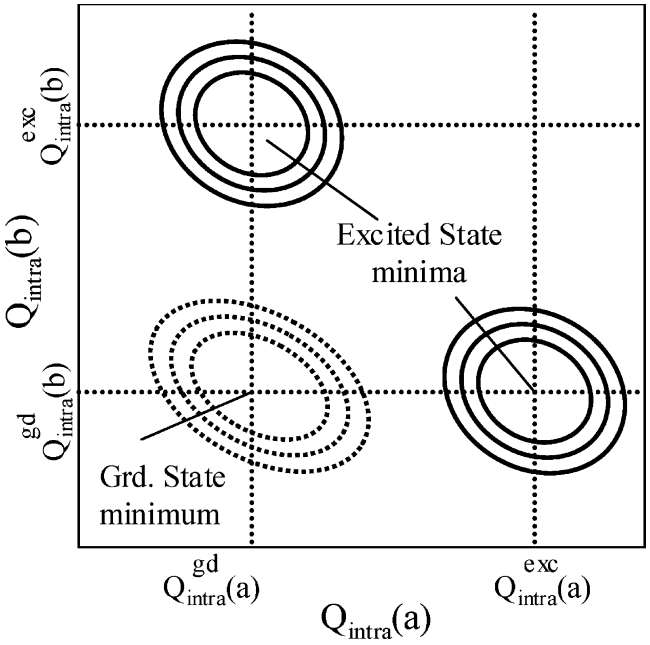

Figure 9. Schematic diagram of potential energy surfaces of the ground state (dashed lines) and excited state (solid lines) of anthranilic acid dimer. The two-dimensional surface shows the two minima created when one of the monomers ("a" or "b") undergoes a large geometry change upon electronic excitation while the other monomer ("b" or "a") retains the ground-state structure.

on the vibrational coordinates. For example, in AA dimer, any excited-state structure with C_{2h} geometry will have two states that can be approximated as

$$\Psi_e^{\pm}(q,Q_a,Q_b) = \frac{1}{\sqrt{2}}(|\psi_a^*\rangle|\psi_b\rangle \pm |\psi_a\rangle|\psi_b^*\rangle) \qquad (1)$$

leading to A_g and B_u symmetry excited states that are delocalized over the two monomer subunits. Here q is used to denote the set of intermolecular coordinates, while Q_a and Q_b are the intramolecular coordinates in monomers "a" and "b", respectively.

However, in the present case, the S_1 state of the AA monomer has a geometry that is substantially different from that of the S_0 state. This will lead to two excited-state minima that are distorted from C_{2h} along the set of intramolecular coordinates Q_a or Q_b, as shown schematically in Figure 9. If the barrier between these two minima is high enough and/or the intramolecular geometry changes are large enough, the electronic excitation will be localized on one of the monomers. In the limit of complete localization, in one well

$$\Psi_e(q,Q_a^{ex},Q_b^{gd}) = |\psi_a^*\rangle|\psi_b\rangle \qquad (2)$$

while in the other

$$\Psi_e(q,Q_a^{gd},Q_b^{ex}) = |\psi_a\rangle|\psi_b^*\rangle \qquad (3)$$

Here Q_a^{gd} and Q_b^{gd} are the values for the intramolecular coordinates at the ground-state minimum structure, and Q_a^{ex} and Q_b^{ex} are the corresponding minimum energy values for the intramolecular coordinates in the excited state. The shift in the locations of the two excited state wells will be along the intramolecular coordinates of only one of the two monomers, either Q_a or Q_b (Figure 9).

In general, at all points on the two excited-state surfaces, a first-order description for the excited states will be

$$\Psi_1(q,Q_a,Q_b) = c_1(q,Q_a,Q_b)|\psi_a^*\rangle|\psi_b\rangle + c_2(q,Q_a,Q_b)|\psi_a\rangle|\psi_b^*\rangle$$

$$\Psi_2(q,Q_a,Q_b) = c_2(q,Q_a,Q_b)|\psi_a^*\rangle|\psi_b\rangle - c_1(q,Q_a,Q_b)|\psi_a\rangle|\psi_b^*\rangle \qquad (4)$$

2. Vibrational Wave Functions. The forms of the vibrational wave functions are also affected by electronic excitation. As mentioned earlier, in the symmetric ground-state structure the intramolecular modes of the dimer are, to a good approximation, in-phase and opposite-phase combinations of the monomer vibrations, leading to closely spaced pairs of vibrations of differing symmetry. For example, the normal modes of the dimer associated with the symmetric stretch of the NH_2 group in the monomer are just sums and differences of the localized NH_2 symmetric stretch coordinates

$$Q_{dim} = \frac{1}{\sqrt{2}}(Q_a \pm Q_b) \qquad (5)$$

which are of a_g and b_u symmetry, respectively. In the usual way, the vibrational wave function for an energy level with v_1 quanta in mode $Q(1)$ and v_2 quanta in $Q(2)$ is then a product of these delocalized wave functions:

$$X_{v_1,v_2}(Q_{dim}(1),Q_{dim}(2)) = \chi_{v_1}(Q_{dim}(1))\,\chi_{v_2}(Q_{dim}(2)) \qquad (6)$$

In the excited state of the dimer, the localization of the electronic excitation on one or the other monomer can produce intramolecular vibrations that are also localized or partially localized on one of the monomer subunits. Normal mode analysis about each of these minima produces two sets of normal modes associated with the two minima. Due to the different structures of the two minima (a·b* and a*·b), the form of the normal modes may be different in the two minima. For instance, in the excited state there are four distinct NH stretch fundamentals, two of which are localized ground-state NH_2 symmetric and antisymmetric stretch coordinates on the ground-state monomer, while the other two involve localized motion of the "free" NH and "dislocated" NH bonds on the electronically excited monomer. In minimum 1 (localized electronic excitation on monomer a), $Q_b^{SS}(1)$, $Q_b^{AS}(1)$, $Q_a^{F}(1)$, and $Q_a^{D}(1)$ are appropriate normal coordinates, while in minimum 2 (localized excitation on monomer b), one should use $Q_a^{SS}(2)$, $Q_a^{AS}(2)$, $Q_b^{F}(2)$, $Q_b^{D}(2)$.

If the barrier separating these two minima is sufficiently large (as we think it is in AA dimer), each vibrational level will be split by a negligibly small tunneling splitting, with vibrational wave functions that are sums and differences of the two localized harmonic wave functions. For example, the tunneling doublet associated with the levels with v_1 quanta in the symmetric NH_2 stretch has vibrational wave functions that are, to a good approximation

$$X_{v_1}(Q^{SS}) = \frac{1}{\sqrt{2}}(\chi_{v_1}(Q_a^{SS}(1)) \pm \chi_{v_1}(Q_b^{SS}(2))) \qquad (7)$$

Similar expressions hold for the other three NH stretch modes. In the excited-state FDIR spectrum, the NH stretch fundamentals are then unresolved doublets associated with excitation out of the a_g and b_u symmetry tunneling doublets to the symmetry-allowed member of the tunneling doublet with $v_{NH} = 1$. Thus,

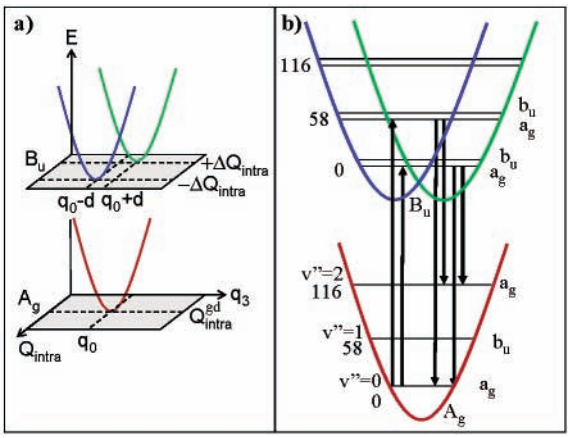

Figure 10. (a) Schematic, two-dimensional potential energy surface for A_g ground electronic state and B_u excited electronic state of AA dimer. The ground-state harmonic well for the geared bend (shown in red) has its minimum at (q_0, Q_{intra}^{gd}), while the two excited-state wells have minima at ($q_0 - d$, $-\Delta Q_{intra}$) and ($q_0 + d$, ΔQ_{intra}), shown in blue and green, respectively. A large barrier separates the two wells in the excited state (not shown), due to the large change in the intramolecular coordinates, Q_{intra}, as the electronic excitation proceeds from localization on one or the other monomer. (b) Schematic energy level diagram of the ground-state and excited-state vibrational levels for the geared intermolecular bend. The three harmonic wells are projected onto a single plane in order to picture the a_g/b_u tunneling doublets that arise in the excited state due to the large barrier that separates the two wells.

the vibrational wave functions are still delocalized over the two wells; however, since all the amplitude is in the region of these two minima where electronic excitation is localized, IR excitation will reflect the localization of the electronic excitation on one or the other monomer.

The intermolecular vibrational energy levels and wave functions are described in a manner similar to that just used for the intramolecular vibrations. The primary difference is that the intermolecular vibrations necessarily involve the motion of both monomer subunits. We are particularly interested in the geared intermolecular bend, which is the third lowest frequency vibration, with normal coordinate label q_3. In the ground electronic state, there is a single minimum, with vibrational wave functions given by $\chi_{v_3}(q_3)$. In the excited state, the two wells still produce wave functions that are localized about the two minima, even if the form of the intermolecular mode is essentially unchanged in the two wells. While the major geometry changes associated with electronic excitation are intramolecular in character, localized electronic excitation will have a secondary effect on the intermolecular vibrations. Figure 10a presents a schematic, two-dimensional potential energy surface in which the full set of intramolecular coordinates that change upon electronic excitation is plotted along one axis $\{Q_{intra}\}$ versus the geared intermolecular bend coordinate q_3. On this two-dimensional surface, the position of the two minima along the q_3 coordinate (shown in blue and green) will be shifted in the excited state by $\pm d$ from the ground-state minimum (shown in red), depending on which monomer is excited; that is, q_3(well 1 in blue) $= q_3^\circ - d$ and q_3(well 2 in green) $= q_3^\circ + d$. Then the vibrational wave functions associated with the geared bend will be sums and differences of these localized harmonic oscillators, producing pairs of levels with a_g and b_u symmetry:

$$X_{v_3}(q_3) = \frac{1}{\sqrt{2}}(\chi_{v_3}(q_3 + d) \pm \chi_{v_3}(q_3 - d)) \qquad (8)$$

Figure 10b projects the three q_3 harmonic wells onto a single plane in order to picture the a_g/b_u tunneling doublets that arise in the excited state due to the large barrier that separates the two wells. Note that the treatment of the wave functions for the geared bend as a sum of localized harmonic oscillators does not depend on the size of d, since the two wells and the height of the barrier separating the two wells are determined primarily by the much larger changes associated with the intramolecular coordinates, Q_{intra}.

This simple model already accounts qualitatively for the anomaly that transitions to $v_3' = 0$, 1, and 2 occur in the excitation spectrum with a spacing of ω_3, while only even overtones appear in the dispersed emission spectra, with a spacing of $2\omega_3$. As the energy level diagram of Figure 10b shows, for a dipole-allowed $B_u \leftarrow A_g$ electronic transition, allowed vibronic transitions out of the ground-state zero-point level (a_g symmetry) will be to the a_g member of each tunneling doublet, producing $v'' = 0 \rightarrow v' = 0$, 1, 2, ... transitions in the excitation spectrum. At the same time, the dispersed emission scans out of these a_g vibrational levels will be only to even overtones of the geared bend in the ground electronic state, as observed.

3. Applying the Model to the Geared Intermolecular Bend Progressions. We have already argued that the model pictured in Figure 10 accounts qualitatively for the transition spacings observed in the excitation and dispersed emission spectra. Here we apply this model quantitatively to the q_3 progressions in the AA dimer spectra. Our starting point is to assume that the geared bend retains its frequency in both ground and excited states (58 cm^{-1}). A quantitative fit of the FC progressions was accomplished by varying the magnitude of the shift d of the excited-state wells relative to the ground state in order to match up with the dispersed emission spectrum from the S_1 origin (Figure 8a). The $\langle v''|v'\rangle$ overlap integrals are a sum of two terms, each of which can be computed in the normal way:

$$\langle X_{v_3''}(q_3)|X_{v_3'}(q_3)\rangle = \frac{1}{\sqrt{2}}(\langle \chi_{v_3''}(q_3^{\,o})|\chi_{v_3'}(q_3^{\,o} + d)\rangle \pm \langle \chi_{v_3''}(q_3^{\,o})|\chi_{v_3'}(q_3^{\,o} - d)\rangle) \qquad (9)$$

Once the magnitude of d was established, it was used to calculate the Franck−Condon profiles for the IR−UV hole-burning spectrum and the other dispersed emission scans involving the geared bend.

Figure 11 presents the best fits to the hole-burning spectrum and the three dispersed emission scans out of the $v' = 0$, 1, and 2 levels in the excited state. The experimental intensity patterns are reproduced for the entire set of data with the shift parameter $D = 1.15$.[35] For the geared bend, this value for D corresponds to a 2.4° angle change (1.2° to either side of zero) between the two geared bend minima in the excited state. An angular change of this magnitude in the geared bend is similar to that deduced for the benzoic acid dimer (3.4°) based on the change in rotational constants upon electronic excitation.[37] This small geometry change along the geared intermolecular bend coordinate means that, if it were not for the shift along other coordinates, the two harmonic wells would "cross" less than 10 cm^{-1} above the bottom of the well, below the zero-point energy ((1/2)(58) = 29 cm^{-1}), as shown in the one-dimensional cuts in Figure 10b. This drives home the point that the small geometry change along the geared bend in the AA dimer is not responsible for the degree of localization of the vibrational wave function along this coordinate, because this localization comes

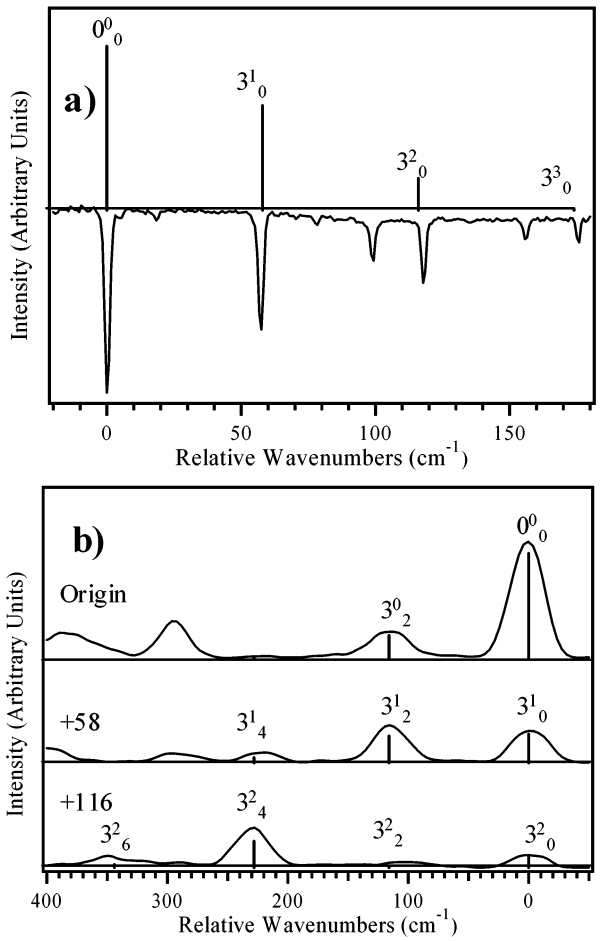

Figure 11. Expanded views of the (a) IR−UV hole-burning spectrum highlighting the progressions in the intermolecular geared bend and (b) the dispersed emission scans from the electronic origin, +58 cm^{-1} band, and +118 cm^{-1} band. The sticks are the best fit to the experimental data using the excited-state model of two shifted harmonic oscillators discussed in the text.

mostly from the intramolecular geometry changes along other coordinates, as shown in Figure 10a.

A few comments regarding the proposed model need to be made. First, the calculations were carried out under the assumption that the excited state is of B_u symmetry, so that the electronic transition ($S_1(B_u) \leftarrow X(A_g)$) is electric dipole allowed. However, there is a second excited electronic state of A_g symmetry, which is nearby in energy. We do not know a priori which state is lower in energy, A_g or B_u. We do know that the S_2 state would nearly touch the S_1 surface at the top of the barrier separating the two minima, somewhere along the diagonal in the schematic potential energy surface of Figure 9. If the S_1 state were of A_g symmetry rather than B_u symmetry, then the b_u symmetry member of the tunneling doublet in Figure 10b would be allowed via vibronic coupling to the B_u S_2 state. To test this possibility, we have carried out calculations of the q_3 progression intensities including vibronic coupling by computing $\langle v''|Q_3|v'\rangle$ matrix elements and varying the shift in the harmonic wells in the same way that was done for the dipole-allowed calculation. However, the intensities in the geared intermolecular bend progressions could not be even qualitatively fit when an A_g upper state was assumed, where the intensities were governed by vibronic coupling. As a result, we deduce that the upper state observed in the present study is of B_u electronic symmetry.

Second, the same type of arguments used to account for the "pure" geared bend progressions should in principle account for the intensities in these bends appearing in the dispersed emission scan of the 99 cm^{-1} band in Figure 8d. However, the same symmetry arguments should not allow the band at 110 + 58 cm^{-1}. We have no explanation for, or assignment of, the emission band at 110 + 58 cm^{-1}, which may simply be an a_g symmetry combination level with no geared bend character.

Finally, it is worth pursuing analogous studies of isotopically substituted AA dimers that have C_s symmetry, such as the $^{14}N/^{15}N$ or NH_2/ND_2 dimers. According to the model proposed here, there will now be two allowed electronic transitions due to $^{14}N^*/^{15}N$ and $^{14}N/^{15}N^*$, which correspond to localized electronic excitation into one of the two wells in Figure 10a. In this circumstance, the excited-state vibrational wave functions in the geared bending levels should be localized in one well, and produce Franck−Condon intensity to both even and odd members of the geared bend in emission.

IV. Conclusions

The excited-state behavior of the hydrogen-bonded dimer of anthranilic acid has been studied with a combination of ultraviolet and infrared spectroscopy. The ground-state infrared spectrum shows an intense, broad OH stretch absorption characteristic of a H-bonded dimer bound together by two OH···O═C H-bonds joining the two carboxylic acid groups. The presence of the amino substituents shuts off the tunneling splitting due to double proton transfer involving the OH···O═C groups, which was present in the benzoic acid dimer.[6] However, these same substituents open the possibility of excited-state hydrogen dislocation involving the NH···O═C group.

Several pieces of spectroscopic evidence support the conclusion that the first excited singlet state of anthranilic acid dimer has a double minimum potential in which the electronic excitation is localized on one or the other monomer in the two wells. This electronic localization is most clearly detected in the excited-state FDIR spectrum in the region between 3400 and 3600 cm^{-1}, in which two of the NH stretch fundamentals are the symmetric and antisymmetric NH_2 stretches of a ground-state monomer, while the third fundamental is the "free NH" characteristic of the excited-state monomer. The vibronic spectroscopy also shows clear evidence for electronic localization in an anomalous set of Franck−Condon profiles involving the b_u symmetry geared intermolecular bend.

The localization of the electronic excitation in anthranilic acid dimer is a dramatic consequence of the large geometry change associated with the excited state of anthranilic acid monomer. We ascribe this large geometry change to the "hydrogen dislocation" in the bound NH bond, which affects the geometry of the entire chelated ring involving the ortho NH_2 and COOH groups.

One can anticipate that the spectroscopic consequences identified here will be quite general manifestations of electronic localization in the excited states of dimers. Any time the excited state of a monomer differs substantially from its ground state, electronic excitation of the homodimer will lead to a double minimum excited state in which the electronic excitation is localized or partially localized on one of the monomers in each well. When the barrier separating these minima is sufficiently large, the vibrational wave functions will reflect the electronic localization as the vibrational wave functions localize around these two minima as well. The intramolecular vibrations may be split if they change character between ground and excited state. The intermolecular vibrations will produce Franck−Condon progressions with intensity patterns characteristic of the double minimum excited state.

Finally, the present results on anthranilic acid dimer bear an interesting relationship to those on benzoic acid dimer. In benzoic acid monomer, electronic excitation to the S_1 state involves a much smaller geometry change ΔQ_{intra}, because the amino group responsible for the H-atom dislocation is no longer present. Hence, one anticipates that the two wells in the dimer will be displaced by a much smaller amount (Figure 10a). This, in turn, will reduce the magnitude of the barrier separating the two wells. In fact, Baum and McClure deduced an exciton splitting of only 0.3 cm^{-1} between the S_1 and S_2 states, with the A_g state below the B_u state.[4] In this case, the displacement along the geared bend coordinate may play a more substantial role in determining the degree of electronic localization in the excited state. In fact, the analogous progressions in the geared intermolecular bend show anomalous intensity patterns, which have not yet been explained adequately. This is an area ripe for further investigation.

Acknowledgment. G.M.F., J.A.S., and T.S.Z. gratefully acknowledge the support of the National Science Foundation under Grant CHE-0242818. J.A.S. thanks NASA for a Graduate Student Research Fellowship.

References and Notes

(1) Baum, J. C.; McClure, D. S. *J. Am. Chem. Soc.* **1979**, *101*, 2335−2339.
(2) Baum, J. C.; McClure, D. S. *J. Am. Chem. Soc.* **1979**, *101*, 2340−2343.
(3) Baum, J. C. *J. Am. Chem. Soc.* **1980**, *102*, 716−719.
(4) Baum, J. C.; McClure, D. S. *J. Am. Chem. Soc.* **1980**, *102*, 720−727.
(5) Florio, G. M.; Sibert, E. L.; Zwier, T. S. *Faraday Discuss.* **2001**, *118*, 315−330.
(6) Remmers, K.; Meerts, W. L.; Ozier, I. *J. Chem. Phys.* **2000**, *112*, 10890−10894.
(7) Poeltl, D. E.; McVey, J. K. *J. Chem. Phys.* **1983**, *78*, 4349−4355.
(8) Poeltl, D. E.; McVey, J. K. *J. Chem. Phys.* **1984**, *80*, 1801−1811.
(9) Tomioka, Y.; Abe, H.; Mikami, N.; Ito, M. *J. Phys. Chem.* **1984**, *88*, 2263−2270.
(10) Bakker, J. M.; Aleese, L. M.; von Helden, G.; Meijer, G. *J. Chem. Phys.* **2003**, *119*, 11180−11185.
(11) Meijer, G.; Devries, M. S.; Hunziker, H. E.; Wendt, H. R. *J. Chem. Phys.* **1990**, *92*, 7625−7635.
(12) Oppenlander, A.; Rambaud, C.; Trommsdorff, H. P.; Vial, J. C. *Phys. Rev. Lett.* **1989**, *63*, 1432−1435.
(13) Rambaud, C.; Trommsdorff, H. P. *Chem. Phys. Lett.* **1999**, *306*, 124−132.
(14) Yahagi, T.; Fujii, A.; Ebata, T.; Mikami, N. *J. Phys. Chem. A* **2001**, *105*, 10673−10680.
(15) Bisht, P. B.; Petek, H.; Yoshihara, K.; Nagashima, U. *J. Chem. Phys.* **1995**, *103*, 5290−5307.
(16) Southern, C. A.; Levy, D. H.; Florio, G. M.; Longarte, A.; Zwier, T. S. *J. Phys. Chem. A* **2003**, *107*, 4032−4040.
(17) Stearns, J. A.; Das, A.; Zwier, T. S. *PCCP Phys. Chem. Chem. Phys.* **2004**, in press.
(18) Lahmani, F.; Zehnacker-Rentien, A. *Chem. Phys. Lett.* **1997**, *271*, 6−14.
(19) Smalley, R. E.; Levy, D. H.; Wharton, L. *J. Chem. Phys.* **1976**, *64*, 3266−3276.
(20) Carrasquillo, E.; Zwier, T. S.; Levy, D. H. *J. Chem. Phys.* **1985**, *83*, 4990−4999.
(21) Ebata, T.; Fujii, A.; Mikami, N. *Int. Rev. Phys. Chem.* **1998**, *17*, 331−361.
(22) Frost, R. K.; Hagemeister, F. C.; Arrington, C. A.; Zwier, T. S.; Jordan, K. D. *J. Chem. Phys.* **1996**, *105*, 2595−2604.
(23) Walther, T.; Bitto, H.; Minton, T. K.; Huber, J. R. *Chem. Phys. Lett.* **1994**, *231*, 64−69.
(24) Frisch, M. J.; Trucks, G. W.; Schlegel, H. B.; Scuseria, G. E.; Robb, M. A.; Cheeseman, J. R.; Zakrzewski, V. G.; Montgomery, J. A., Jr.; Stratmann, R. E.; Burant, J. C.; Dapprich, S.; Millam, J. M.; Daniels, A. D.; Kudin, K. N.; Strain, M. C.; Farkas, O.; Tomasi, J.; Barone, V.; Cossi, M.; Cammi, R.; Mennucci, B.; Pomelli, C.; Adamo, C.; Clifford, S.; Ochterski, J.; Petersson, G. A.; Ayala, P. Y.; Cui, Q.; Morokuma, K.; Malick, D. K.; Rabuck, A. D.; Raghavachari, K.; Foresman, J. B.; Cioslowski, J.; Ortiz, J. V.; Baboul, A. G.; Stefanov, B. B.; Liu, G.; Liashenko, A.; Piskorz, P.; Komaromi, I.; Gomperts, R.; Martin, R. L.; Fox, D. J.; Keith, T.; Al-Laham, M. A.; Peng, C. Y.; Nanayakkara, A.; Challacombe, M.; Gill, P. M. W.; Johnson, B.; Chen, W.; Wong, M. W.; Andres, J. L.; Gonzalez, C.; Head-Gordon, M.; Replogle, E. S.; Pople, J. A. *Gaussian 98*, revision A.9; Gaussian, Inc.: Pittsburgh, PA, 1998.
(25) Meijer, G.; Devries, M. S.; Hunziker, H. E.; Wendt, H. R. *J. Phys. Chem.* **1990**, *94*, 4394−4396.
(26) Wilson, E. B. *Phys. Rev.* **1934**, *45*, 706−714.
(27) Florio, G. M.; Zwier, T. S.; Myshakin, E. M.; Jordan, K. D.; Sibert, E. L. *J. Chem. Phys.* **2003**, *118*, 1735−1746.
(28) Fuke, K.; Yoshiuchi, H.; Kaya, K. *J. Phys. Chem.* **1984**, *88*, 5840−5844.
(29) Fuke, K.; Kaya, K. *J. Phys. Chem.* **1989**, *93*, 614−621.
(30) Taylor, C. A.; El-Bayoumi, M. A.; Kasha, M. *Proc. Natl. Acad. Sci. U.S.A.* **1969**, *63*, 253−260.
(31) Catalan, J.; Kasha, M. *J. Phys. Chem. A* **2000**, *104*, 10812−10820.
(32) Lahmani, F.; Zehnacker-Rentien, A. *J. Phys. Chem. A* **1997**, *101*, 6141−6147.
(33) Sobolewski, A. L.; Domcke, W. *Chem. Phys.* **1998**, *232*, 257−265.
(34) Sobolewski, A. L.; Domcke, W. *PCCP Phys. Chem. Chem. Phys.* **1999**, *1*, 3065−3072.
(35) Henderson, J. R.; Muramoto, M.; Willett, R. A. *J. Chem. Phys.* **1964**, *41*, 580−581. In the notation used in this paper, $D = \alpha\Delta$, where $\alpha = (\omega/\hbar)^{1/2}$ and Δ is the normal coordinate shift equivalent to *d* in this work.
(36) Müller, A.; Talbot, F.; Leutwyler, S. *J. Chem. Phys.* **2002**, *116*, 2836−2847.
(37) In Remmers et al. (ref 6), the magnitude of the shift along q_3 is defined by the angle α formed by the *a* inertial axis of the ground-state C_{2h} dimer and the line connecting the center of mass of the dimer to the center of mass of one monomer unit in the bent excited-state geometry. In the present work, α is defined as the angle between the line connecting C2 and C3 of one monomer unit (see Figure 3) in the C_{2h} geometry, and the same line in the bent geometry. In benzoic acid dimer, these two definitions are equivalent, but in anthranilic acid dimer they are not due to the presence of the NH_2 groups, which rotate the *a* inertial axis off the C_2–C_3 axis.